A Compact Dual Bandpass Filter Using Dual Composite Right-/Left-Handed and Open-Loop Ring Resonators for 4G and 5G Applications

Xuan Phuc DAO [1], Van Son NGUYEN [1], Van Dung TRAN [2], Thanh Trung VU [2], The Hoang NGUYEN [2], Xuan Loi DAI [3], Nghia Hoang TRONG [1], Tran Tuan LINH [1]

[1] Faculty of Electrical and Electronic Engineering, Hanoi Open University (HOU), 100000 Hanoi, Vietnam
[2] Institute for Technology Development Media and Community Assistance (IMC), 100000 Hanoi, Vietnam
[3] Military Institute of Science and Technology, 100000 Hanoi, Vietnam

{phucdx, sonnv}@hou.edu.vn, {dung.tranvan, trung.vuthanh, hoang.nguyenthe}@imc.org.vn, daixuanloi@gmail.com, nghiaht19@gmail.com, 23a1201d0161@students.hou.edu.vn

Submitted October 5, 2023 / Accepted February 22, 2024 / Online first March 11, 2024

Abstract. *In this paper a very compact design of a dual-band band pass filter (D-BPF) using dual composite right-/left-handed (D-CRLH) and open-loop ring (OLR) resonators is presented. To overcome the frequency ratio limitations of D-CLRH resonators technique, the D-BPF design combines D-CRLH and OLR resonators to finally perform a D-BPF. The filter covers the 2.6 and 3.5 GHz spectrums for 4G and 5G applications, respectively. The reported D-BPF is designed and optimized using ADS software, and is implemented on a Rogers RO5880 substrate with a relative dielectric constant of 2.2 and thickness of 0.787 mm. The overall compact size is 8 × 8 × 0.787 mm³. To our knowledge, this design is considered as the most compact and smallest size dual-bandpass filters.*

Keywords

Band pass filters (BPFs), dual-band band pass filters (D-BPFs), dual composite right-/left-handed (D-CRLH), open-loop ring (OLR), bandwidth (BW), 4G, 5G applications, compact size

1. Introduction

The deployment of 5G wireless communication applications has been employing in recent years. In many countries, the 6 GHz sub-band (mid-band) is planned and employed for the 5G network. The 5G NR bands used in most Asian nations, such as Vietnam in these bands are n41 (2.496–2.690 GHz) and n78 (3.3–3.8 GHz) [1].

Microstrip dual-band bandpass filters play an important role in an RF receiver, especially in the newly developed 5G wireless communication networks. To overcome challenges about bandwidth, unwanted signals, and noise, D-BPFs are necessary to simultaneously suppress undesirable signals and select the desirable signals in different frequency bands and bandwidths (BWs) [2–4].

The challenges to designing a D-BPF are how to achieve high passband selectivity, better performances, and larger bandwidth [4], [5]. The technology used behind D-BPFs decides how to achieve compact size and better performances. Many microwave designers have been studying different methods to get the best D-BPF [5–24].

Stepped impedance resonators (SIRs) are a popular method to design a D-BPF, but they have drawbacks such as difficulty in creating the second passband and large layout. Also, it would be a big challenge to control the passbands independently by using the SIR, as the dual passbands response is synthesized by the two resonator responses synchronously [5–9].

Another method uses modified coupled-line structures and step-impedance open-circuited stubs, which can extend the bandwidth, but also occupy a large area. Open/short-circuited stubs can also be used to construct a dual-band filter, but they consume a large area as well [10]. In [3] the microstrip BPF combines four open-loop ring resonators to achieve sharper cut-off frequencies. The utilization of the planar four-section resonators can provide either positive or negative cross-coupling. The process of designing the filter is very simple with a simply structure. However, these structures properly consume a large area as more than one quarter-wavelength resonators represented in the design.

Dual-mode resonators such as square loop, stub-loaded, and microstrip patch, circular disk resonators are another basic technique, but they have complex layouts and poor performance [11–16].

Combining two single-band filters is a common way to perform a D-BPF, but it also faces the challenge of size reduction and performance optimization due to the additional impedance-matching networks as well as the presentations of more than one quarter-wavelength stub [16], [17].

DOI: 10.13164/re.2024.0213

There is a potential candidate to reduce size of a D-BPF while fulfilling other requirements. It is the use of dual CRLH configuration. The advantages of this technique is to miniaturize the microwave devices. Then, many works with the improvement in structure and better performance are constructed based on this theory [17–19]. Using dual CRLH resonators, an analytical design method of compact DBFs is investigated in [20], [21]. In these works, the group of authors also show 88% size reduction of the proposed structure compared with the published dual-band BPFs.

The proposed design method can independently and flexibly control the center frequencies, BWs, and coupling coefficients of D-BPFs. As the result, the impedance matching of the filter can be easily attained. The valid range of center frequency ratio is from 1.6 to 3.11. Compared to other works in [2–24] the valid ranges of center frequency and BW ratios in [20], [21] are much larger.

However, there are two main points that must be highlighted here. Firstly, the frequency ratio is still not enough to propose a D-BPF having two center frequencies close to each other. For example, 2.6 GHz (n78) and 3.5 GHz (n41) are two close frequencies which cannot be designed based on the dual CRLH resonators technique. The range of center frequency ratio is 1.35 (3.5/2.6) which is out of the valid range (1.6–3.11).

To clarify the limitations of this method, a dual-band filter design using this dual band CRLH resonators technique at 2.6 and 3.5 GHz is simulated in ADS.

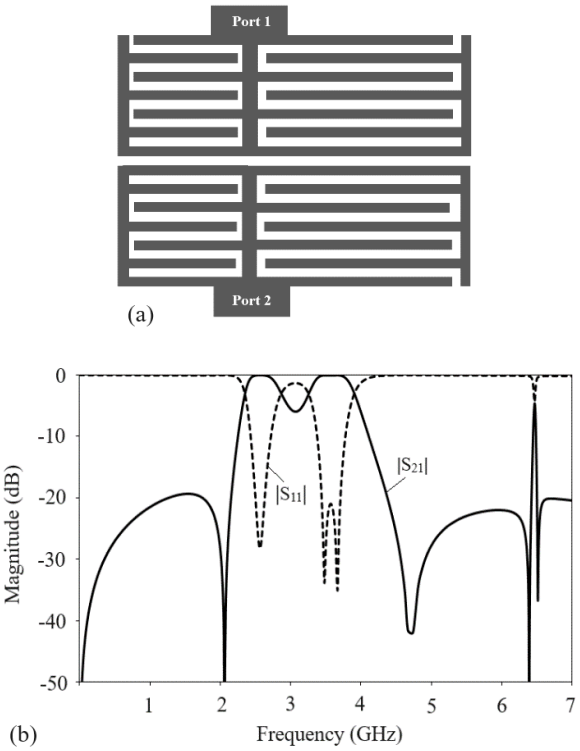

Fig. 1. A design example of the D-BPF with the frequency ratio being 1.35: (a) Overall structure; (b) S-parameter simulation.

As shown in Fig. 1(b), S-parameters somehow meet the requirements for a D-BPF. However, the stopband rejection between two passbands at center frequencies (2.6 and 3.5 GHz) is 8 dB. It is much smaller than an acceptable value of 25 dB. We expected that the center frequency ratio would be as small as possible with the stopband rejection larger than 25 dB. So, this technique is not usable in designing a D-BPF.

Secondly, the size of proposed filters in [20], [21] could be reduced more when we combine D-CRLH and OLR resonators in a compact design. To overcome the limitation of the D-CRLH technique while still maintaining its advantages, a design is proposed by combining two techniques. The first band pass filter is executed to get the smaller size and compact shape with higher selectivity using a D-CRLH resonator. The second band pass filter is finally achieved by adding the open loop ring resonator surrounding the first band. The combination between two techniques can help to fulfill all requirements, especially a very compact size.

In this work, a very compact DBF with a simple design procedure is presented for 5G band occupying the range of 2.6–3.5 GHz.

The structure consists of a CRLH and OLR resonators. The organization of this paper is as follows. Section 1 provides an overview of dual band pass filters and the literature providing mainly real relevant state of the art in the field. In this section, the proposed D-CRLH resonator filter and its limitations are highlighted based on one simulated example designs to propose a new combination technique for our work. Section 2 provides a proposed methodology. Two design examples are presented in Sec. 3 following by the discussion of the results. Finally, the conclusions are given in Sec. 4.

2. Methodology

The procedures of the proposed design method include four main steps.

Step 1. Determine the desired specifications of the dual-band filter.

In this step, we first choose the suitable types of resonators for each center frequency of a D-BPF. Then, two center frequencies are stuck with the CRLH and OLR resonators, respectively.

Step 2. Design the first band filter using the CRLH technique.

The D-CRLH unit cell is optimized with the accurate equivalent circuit sticking with the desired center frequencies (the first resonator frequency) and fractional bandwidth.

Step 3. Design the second band filter using the OLR resonator.

After step 2, a first band filter is proposed. Then, the open-loop ring resonators are added to meet the desired

response requirements of the second band filter. It is simple to determine the structural design of the OLR resonator. The length of the resonator is selected to be $\lambda_g/2$, where λ_g characterizes the guided wavelength at the second resonant frequency. The width of the resonator does not have much impact on the overall performance.

Step 4. Adjusting the coupling coefficients between the D-CRLH resonators and the OLR resonators.

It is crucial to determine the shape of the OLR resonator to achieve the requirement expectation. The $\lambda_g/2$ resonator needs to be bent around the CRLH resonator to achieve the compact size. Tuning the spacing between the first band resonators and OLR resonators to optimize the desired specifications is necessary. This spacing will decide the fractional bandwidth of the second resonator frequency and upper stopband rejection.

The design procedure of a novel dual CRLH resonator (step 2) is presented in [20], [21]. In our work, we only try to present step 3 and step 4 most simply. It is a complex process to design a BPF using the CRLH technique. To simplify the technique mentioned in [20], [21], we highlight some main points as below. The D-CRLH structure is a combination of an interdigital capacitor and a shunt metallic line at both sides to perform a single-mode D-CRLH resonator, as shown in Fig. 2(a).

The interdigital capacitor consists of many microstrip lines. The fingers provide coupling between the input and output ports across the gaps. N_p is the number of finger pairs. The more fingers the interdigital capacitor has, the more fractional bandwidth the filter will be. The length (L) and width (W_1) of the capacitor are tunable (changing the value of the interdigital capacitor) to define the center frequency. Parameters S_e and S_0 are the gaps between each finger and at the end of the finger. W_f is the width of the in-out ports that decides the value of S_{11}. The shunt metallic line

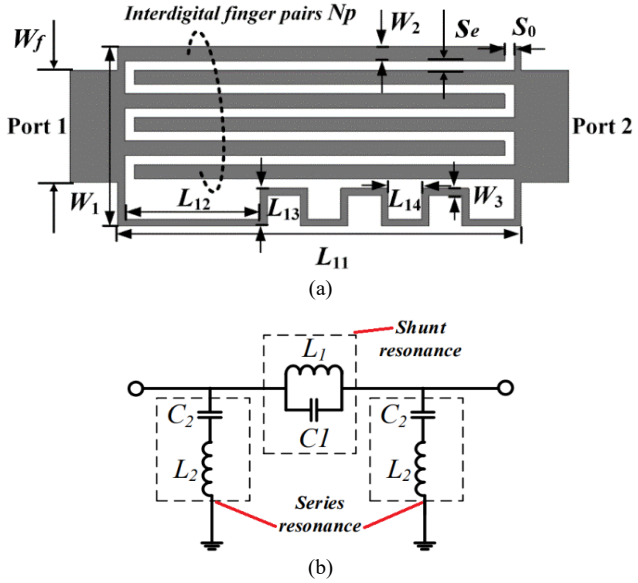

Fig. 2. Single-mode D-CRLH resonator. (a) Schematic layout. (b) Equivalent circuit model [20], [21].

is proposed by its shape with some parameters, namely, L_{12}, L_{13}, L_{14}, and W_3.

So, there are 11 structural parameters of the single-mode D-CRLH resonator that need to be tuned for optimization.

It is necessary to reduce 11 parameters to reduce the complexity of the technique. Typically, the gaps S_e and S_0 are the same to simplify the design. The width of the finger should be equal to the gaps. To achieve a compact and small size, the finger's width needs to be reduced. However, as the limitation of the precision machines, the minimum W_2, S_e, and S_0 should be greater than 0.15 mm. Then, instead of using a bent and folded shunt metallic line, it can be replaced by a straight line to eliminate the L_{12}, L_{13}, and L_{14} parameters of the inductor. The inductor's width can be chosen the same as the finger's width ($W_3 = W_2$). The length of the inductor is reduced, and the length of the capacitor's finger will be increased.

As a result, there are only some main variable quantities for the resonator, including L, W_1, W_2, S_0, and N_p as they are indicated in Fig. 3(a). With the help of the simulation EM function in ADS, it is easier for designers to optimize and achieve the design expectations.

Figure 2(b) shows equivalent circuit model for the D-CRLH resonator unit cell. The resonant frequencies and BWs of the first passband depend mainly on the values of C_1 and L_1 where C_1 and L_1 represent the capacitance of the interdigital capacitor and inductance of the shunt metallic line, respectively. The relation among these characteristics is presented by the following equations:

$$f = \frac{1}{2\pi L_1 C_1}, \tag{1}$$

$$FBW = \frac{\sqrt{L_1 C_1^{-1}}}{R_1}. \tag{2}$$

R_1 is the series D-CRLH resonator's attenuation effect. Different combinations of (L_1 and C_1) with constant $L_1 \times C_1$ allow for independent control of the bandwidth for the first passband.

The circuit model can be input into the ADS to optimize the capacitance and inductance to obtain the optimal dimensions. Based on the extracted parameters as well as the empirical formulas of the interdigital capacitor and high impedance line, the initial values of the dimensions can be estimated.

The two single-mode resonators are cascaded to perform a dual-mode D-CRLH resonator as shown in Fig. 3(a). At this step, one new structural parameter of interest is the gap or spacing between two single-mode resonators (G). Spacing G is the main factor affecting the coupling coefficients of the resonator A and B. By keeping G constant, the coupling coefficient remains stable. This makes it easy to achieve good impedance matching by choosing a suitable G.

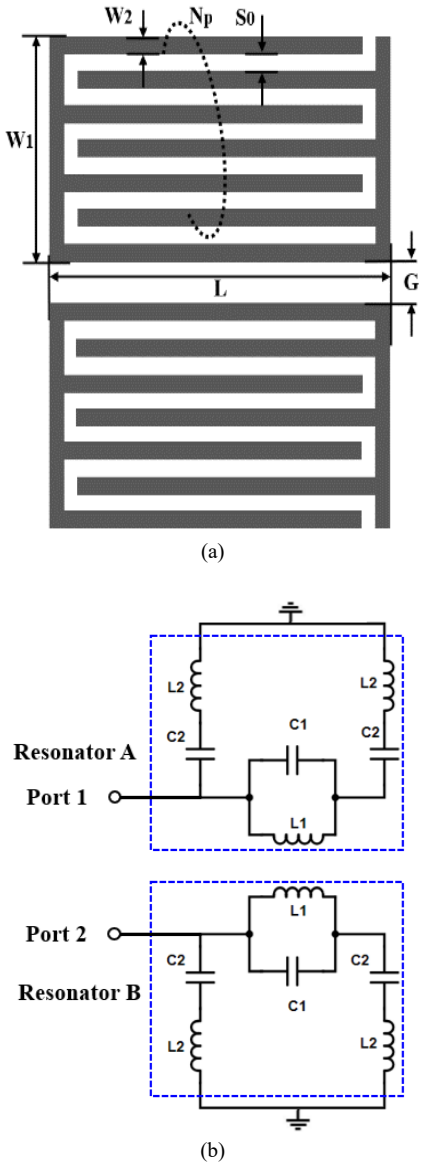

Fig. 3. Dual-mode D-CRLH resonator. (a) Schematic layout. (b) Equivalent circuit model.

Finally, there are 6 interest parameters deciding the overall performance of the first passband filter as they are shown in Fig. 3(a) compared to 11 parameters in [20], [21].

As the conductors of filters are mounted on a substrate, their characteristics therefore affect the overall performance. For a PCB, the dielectric constant (ε_r) has the most impact on the electrical characteristics of the filter design. To achieve low loss and minimum difference between simulated and fabricated PCB layout filter designs, Rogers RO5880 substrate with a relative dielectric of 2.2 and thickness of 0.787 mm is chosen. The minimum width and spacing of each physical piece is 0.2 mm for the exact requirements of size deviation and tolerance machining. To reduce cost, we highly recommend another material of Rogers RO4350B for the substrate.

3. Result and Discussion

3.1 Circuit Design

The design procedure will be further explained by designing an example of dual-band filters. The center frequencies of the two passbands are 2.6 GHz (n41) and 3.5 GHz (n78), and the center frequency ratio is around 1.35. Following the design procedures mentioned above, we first define two center frequencies with the CRLH and OLR resonators, respectively. The 2.6 GHz band is selected as the first band using a D-CRLH resonator. The remaining frequency (3.5 GHz) is chosen as the second band by the OLR resonator technique.

Based on this theory mentioned in [20], [21] and a simple summary of the methodology, a very compact D-CRLH filter is designed. The schematic of the D-CRLH filter is derived from its equivalent circuit model and shown in Fig. 4(a). A single mode resonator is composed of a MICAP capacitor and a MLIN inductor. To simplify the design, we set all the capacitor parameters G, G_e, W_t, W_f to be equal. We only vary two parameters (a, b) that correspond to the length of the inductor and the MICAP capacitor. We adjust them to achieve the desired S-parameter performance at the center frequency of 2.6 GHz, as shown in Fig. 4(b).

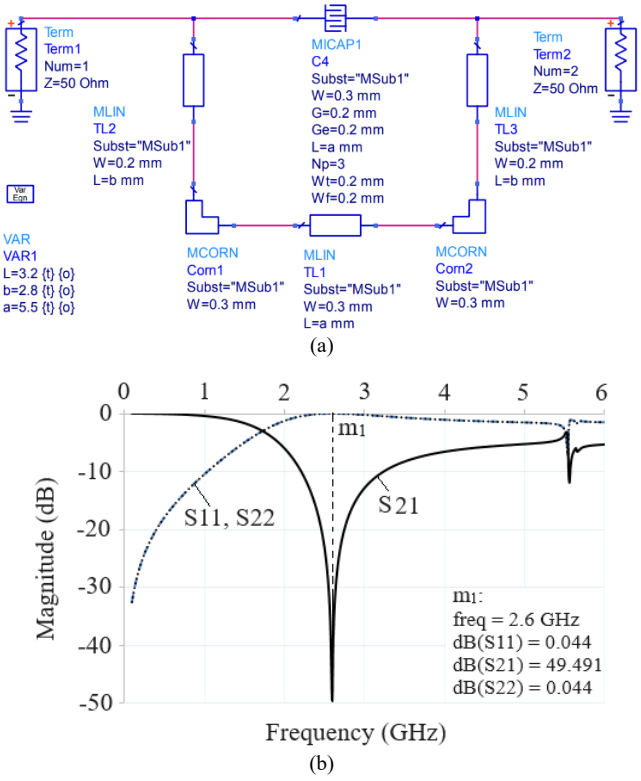

Fig. 4. The schematic (a) and its simulation (b) of one single-mode resonator.

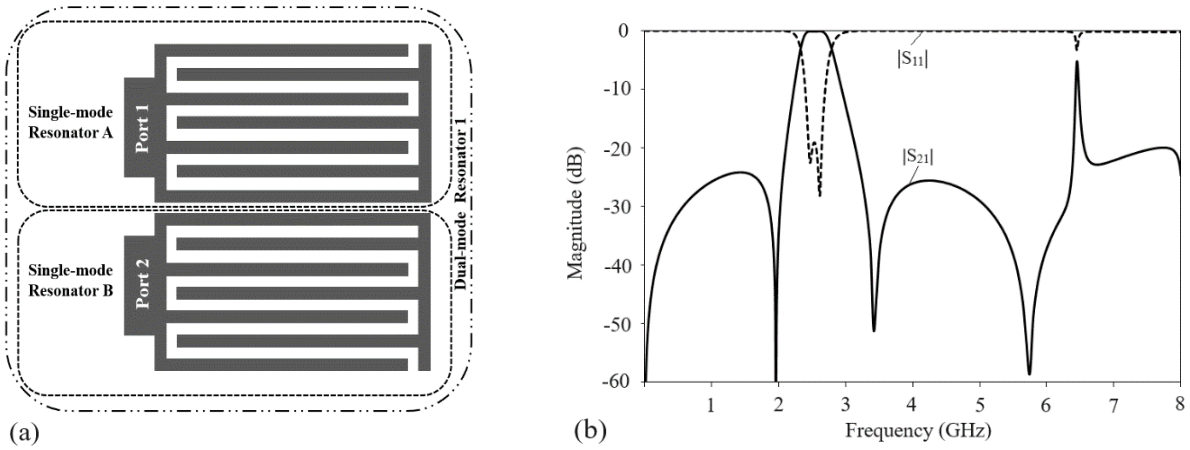

Fig. 5. The geometrical structure of the first bandpass filter with the D-CRLH resonator at a center frequency of 2.6 GHz band (a) and simulation results (b).

W_1	W_2	S_0	L_1	N_p	G	S_1	S_2	S_3	S_4	L
3.4	0.3	0.2	7	6	0.35	0.2	0.2	0.2	0.4	38

Tab. 1. Dimensions of the D-BPF (in mm).

We construct a dual-mode resonator from two single-mode resonators A and B, as shown in Fig. 5(a). The gap G is the coupling coefficient that affects the impedance matching significantly. Also, coupling coefficient will influence BW. Therefore, we need to adjust the gap G between the two resonators to obtain a good S-parameter performance.

The dimensions of the filter are estimated and listed in Tab. 1.

As can be seen in Fig. 5(b), the second-order filter has a sharp selectivity with two transmission zeroes near the passband. The simulated return loss and insertion loss are 0.1 and below –20 dB. The fractional bandwidth is 250 MHz covering the frequency range of 2.45 GHz to 2.7 GHz. Transmission on zeroes (GHz) is at 1.96 and 6.4. Upper stopband rejection (–25 dB) is 4.32 (6.4/1.48). The harmonic appears at 6.4 GHz, indicating that this filter has 25 dB upper stopband rejection till $2.46f_0$. The simulated insertion loss is 0.1 dB.

To achieve dual-band characteristics, resonator 3 is added to the second-order filter. The equivalent elements of D-CRLH resonator and OLR resonator are shown in Fig. 6.

Resonator 3 is the OLR with the shape being bent around resonators A and B to achieve the compact size as it is shown in Fig. 6. There are two main parameters of the resonators which primarily decide the performance of the second band. First, the length of the resonator 3 is selected to be $\lambda_g/2$, where λ_g represents the guided wavelength at the resonant frequency of 3.5 GHz:

$$\lambda_g = \frac{300}{f\sqrt{\varepsilon_{\text{eff}}}}. \tag{3}$$

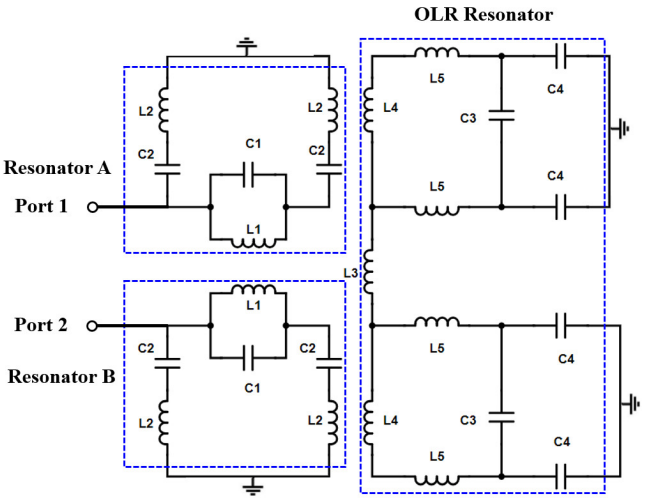

Fig. 6. The equivalent circuit for the proposed dual-band filters combining a D-CRLH resonator and OLR resonator.

In (3) ε_{eff} is dielectric constant and equal to 2.2 and f is frequency in GHz [22], [23]. So, the total length of the line is 58 mm with $\lambda_g/2$ being 29 mm. Then, the length must be tuned and simulated in ADS to optimize the parameters. The actual length of the OLR resonator after optimizing is around 38 mm. Second, the gaps between the first band filter and the OLR resonator (S_2 and S_4) have a huge impact on the S-parameters of the second band as well as the over-all D-BPF design. At this step, there are some ways to bend the OLR resonator around the first band filter. The gaps are also differently tuned to achieve a specific expectation. There are 2 versions as shown in Fig. 7 below.

For example, in Filter I, the main line is bent into 7 smaller lines around the resonators 1 and 2 to minimize the overall space of the dual-band filter and, therefore, achieve the compact size. S_1 and S_2 or S_3 and S_4 are the spaces

between the first band filter and the OLR resonator. These parameters are optimized to achieve the fractional bandwidth and S-parameter of the second passband as well as the overall S-parameter of the D-BPF. For the second version, the transmission line is bent as a spiral inductor. The length of each spiral line is simply determined based on the way they are bent around the previous resonator and the defined total length.

To simplify the design procedure, we choose the width of the OLR resonator equal to the width of the first resonator ($W_2 = 0.3$ mm). Figure 7 shows the configuration of the designed BPF combining 2 different techniques. Obviously, the size of the designed filter is very compact. The optimized parameters are obtained by using the EM Simulator in the ADS environment to achieve a good performance of S-parameter as they are indicated in Fig. 10.

The overall size of Filters I and II shown in Fig. 7 are 7×9 mm^2 and 8×8 mm^2, respectively. The size of the resonator is very compact with only $0.058\lambda_g \times 0.077\lambda_g$ and $0.068\lambda_g \times 0.068\lambda_g$, where λ_g is the guided wavelength of 50-Ohm microstrip at center frequency for the first band (2.55 GHz).

3.2 Measurement Result

The proposed D-BPF is implemented on a Rogers RO5880 PCB with a relative dielectric constant of 2.2 and thickness of 0.787 mm. The final structural dimensions and the layout of the proposed D-CRLH and OLR resonators dual-band filter are shown in Fig. 8.

To facilitate the measurement process, input and output ports are bent and expanded to the 50-Ohm SMA connection. As there is an outer-resonator coupling between the ports and assembled resonators, it is necessary to calculate how it effects on the overall S-parameter by optimizing in ADS.

The measurement is carried out using an E5080B ENA Vector Network Analyzer to obtain the S-parameter of design. The measurement set-up is shown in Fig. 9. The Keysight RF electronic calibration (ECal) module is first used to make calibration of vector network analyzers fast, easy, and accurate. This step is very important to maintain accuracy, standardization, and repeatability in measurements, assuring reliable benchmarks and results.

The S-parameter simulation and measured results of Filters I and II are shown in Fig. 10 and summarized in Tab. 2.

Figure 10(a) shows the S-parameter simulation and measured results of Filter I. For the first passband, it can be seen that the measured center frequency is 2.62 GHz with minimum insertion loss, return loss, and 3-dB fractional BW of 1.19 dB, 18 dB, and 11%, respectively. The first band has a sharp selectivity (50-dB attenuation) with transmission zeroes near the passband at 1.94 GHz.

For the second band, the center frequency is 3.55 GHz while minimum insertion loss and return loss are 1.14 dB and 20 dB, respectively. The 3-dB fractional BW is 3.2% from 3.45 to 3.56 GHz. The stopband rejection between two passbands is larger than 30 dB, peaking at the lowest point of 32 dB. The transmission zeroes are positioned at 5.1 GHz with more than 25-dB attenuation, respectively. The simulated and measured center frequency ratio is 1.35.

Figure 10(b) shows the measured insertion loss (S_{21}), and input (S_{11}) return loss of example II. The simulated and measured insertion loss of the first and second bands is approximately 0.9 and 1.4 dB in the 2.41–2.7 GHz band and 3.45–3.55 GHz, respectively. The 3-dB fractional bandwidths are 12% and 3.1%, correspondingly. For both two

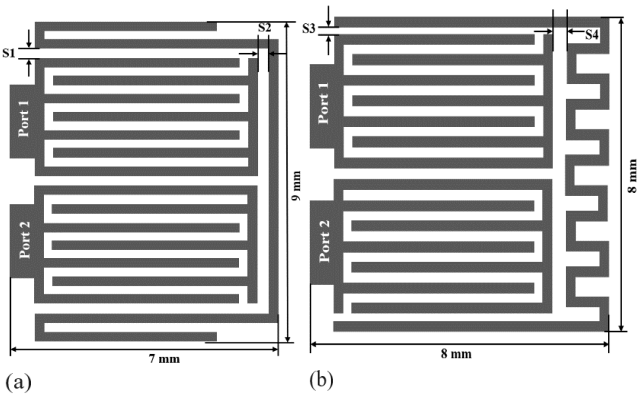

Fig. 7. The layout of Filter I (a) and Filter II (b) of the D-BPF.

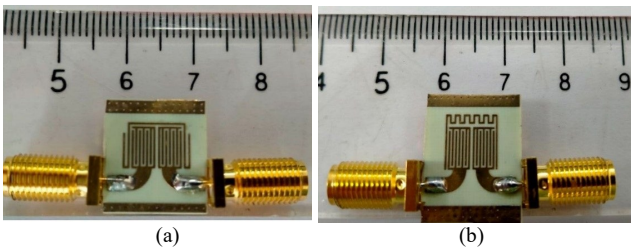

Fig. 8. The structure layout of Filter I (a) and Filter II (b).

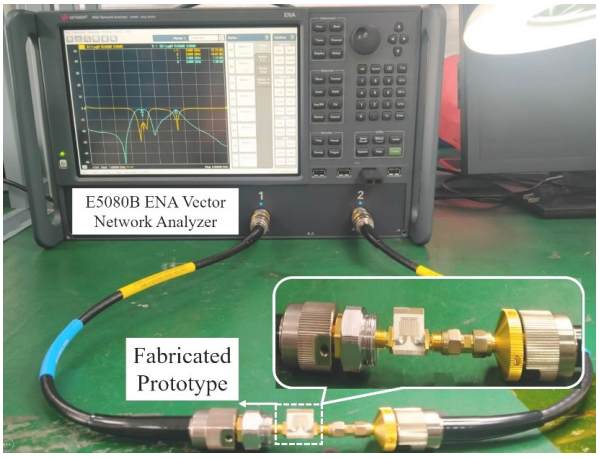

Fig. 9. The measurement set-up.

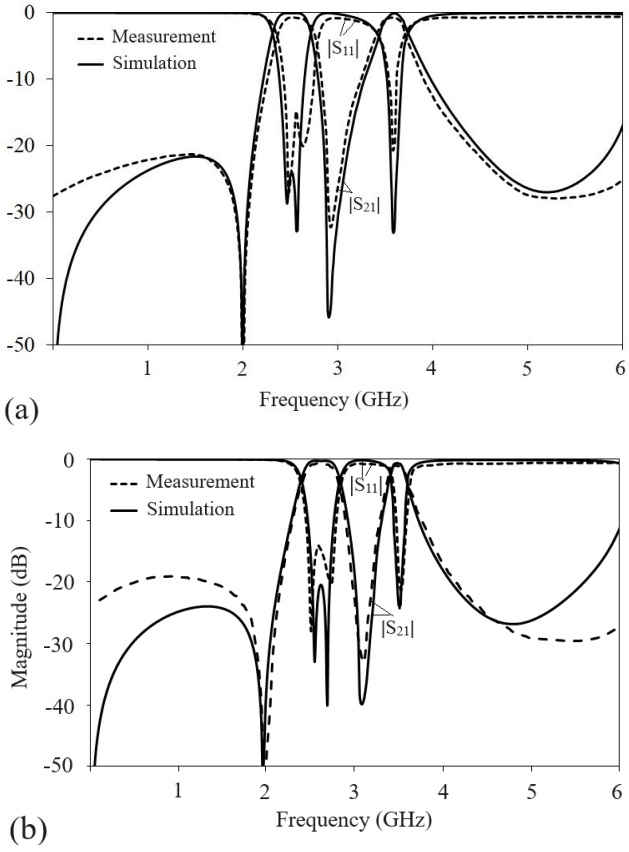

Fig. 10. S-parameter simulation (solid line) and measured (dashed line) results of Filter I (a) and Filter II (b).

passbands, the input and output return losses are better than 15 dB.

The stopband rejection between two passbands is larger than 30 dB, peaking at the lowest point of 40 dB. Two transmission zeroes are positioned at 1.94 and 4.8 GHz with more than 50-dB and 25-dB attenuation, respectively. The simulated and measured center frequency ratio is 1.35. Overall, there is not much difference between simulations and measurements. The contrast between simulated and measured insertion loss is under 0.6 dB in the fractional bandwidth. It is highlighted that the S-parameter performance of the first band D-BPF as shown in Fig. 10 for both Filter I and II is a bit different from its simulation results of the D-CRLH filter in Fig. 5(b) with the appearance of OLR resonator and its coupling coefficient.

Filter II has a smaller fractional BW of the second passband compared to Filter I. However, transmission zeroes at the second band are lower positioned at 4.8 GHz compared to 5.2 GHz. With the closer transmission zeroes appearing near the second passband edges, a good band selectivity for the second passbands can be easily obtained. For both design examples, with the use of an OLR resonator, the 3-dB fractional BW of the second passband is smaller than that for the D-CRLH resonator passband, an average of 100 MHz compared to 280 MHz. The small deviation of 0.6 dB between simulation and measurement results is mainly due to radiation loss and mismatching between SMA connectors.

3.3 Discussion

In this analysis, the initial goal is to achieve the most compact design with minimum size. At the same time, the proposed technique needs to overcome frequency ratio limitations of the dual composite right-/left-handed (D-CLRH) resonators technique. Two versions of the D-BPF are mentioned. The main performances and overall size of the filters are compared. The results are summarized in Tab. 2. Most publicized designs mentioned in Tab. 2 have the same center frequencies band with our work for comparison.

It can be seen that the proposed D-BPFs are significantly compact with size reduction of over 90%. The structure consists of composite right-/left-handed and open-loop ring resonators. With the addition of OLR resonator, the valid range of center frequency ratio is expanded to 1.35. The ratio is smaller than the range in [20], [21] meaning that this technique can be widely used no matter what the frequency ratio is. The valid ranges for the proposed filters are also much larger than those of previously published works in Tab. 2. Therefore, it is easy to control the center frequency with a large flexibility. The first is separated from the second band making it convenient for obtaining the derivable frequencies.

Compared with the D-CRLH resonator technique, the combination of D-CRLH and OLR resonators remains the same selectivity and stopband suppression for the first band, but a much better size reduction is achieved. To our knowledge, this is considered the most compact and smallest size dual-bandpass filter with the center frequency ratio being very low. All results reflect the advantages of this technique compared to other techniques regarding its compact size.

In summary, to achieve the results as shown in Fig. 10, we need to follow 4 steps mentioned in Sec. 3. First, a single-mode resonator is designed at 2.6 GHz using D-CLRH technique. The dimensions of the MICAP and MLIN inductor are tuned to get the optimized parameter in Fig. 4(b). Next, a dual-mode resonator is formed from two single-mode resonators as they are shown in Fig. 5(a). In this step, the gap G between 2 resonators is tuned to achieve optimal performances. There is a difficulty to achieve expected values of S-parameters as there are many variables for tuning. However, it is easier to preserve dimension of the MICAP while the length of the wire inductor can be changed. The simulation results with optimal performances are shown in Fig. 5(b).

After achieving the single pass band filter, one OLR resonator is added. To get the final result as seen in Fig. 10, the spacing between the D-CRLH and OLR resonators G is carefully tuned. This parameter determines the fractional bandwidth of the second resonator frequency and upper stopband rejection, while the length and shape of the OLR resonator have a minor effect. The length of the OLR resonator only affects the center frequency of the second pass band.

Designs	Center frequency f_1 / f_2 (GHz)	Ratio frequency r_f	FBW (%)	Return losses R_{La}/ R_{Lb} (dB)	Insertion loses I_{La}/ I_{Lb} (dB)	Size ($\lambda_g \times \lambda_g$)
Ref. [3]	2.6 / 3.7	1.42	4 / 2.7	13 / 12	1.2 / 2	0.3 × 0.25
Ref. [5]	2.4 / 5.7	2.38	6 / 7	15 / 12	0.5 / 2.2	0.27 × 0.30
Ref. [9]	3.65 / 2.55	1.54	12.5 / 10.8	21 / 28	0.4 / 1.7	0.25 × 0.3
Ref. [10]	2.6 / 5	1.92	31 / 15	18 / 15	0.8 / 1.7	0.59 × 0.89
Ref. [14]	2.4 / 5.2	2.17	9.2 / 9.5	18 / 15	1.4 / 2.7	0.18 × 0.18
Ref. [15]	2.55 / 3.65	1.43	6.7 / 5.2	21 / 12	1.22 / 2.13	0.29 × 0.41
Ref. [20]	2.48 / 1.21	2.04	26 / 10	20 / 25	0.6 / 0.43	0.05 × 0.094
Ref. [24]	2.5 / 3.8	1.52	8 / 9	23 / 25	1 / 2	0.25 × 0.37
Filter I	2.6 / 3.5	1.35	11 / 3.2	18 / 20	1.1 / 1.2	0.058 × 0.077
Filter II	2.6 / 3.5	1.35	12 / 3.1	16 / 18	0.9 / 1.4	0.068 × 0.068

Tab. 2. Comparison between the proposed filters and filters in references.

4. Conclusion

In this work, a very compact and small-size D-BPF with a simple design procedure is presented for 4G and 5G applications. The circuit configuration is composed of D-CRLH and OLR resonators. The first band for the n41-5G band is performed by D-CRLH resonators while the second for the n78-5G band is created by adding OLR resonators.

The measured results of the two samples show a good agreement with simulations. The center frequency bands are 2.6 and 3.5 GHz with minimum insertion loss, and return loss of 1.1 to 1.4 dB (S_{21}) and 20 dB (S_{11}), respectively. The bandwidths of the first and second bands are 280 and 110 MHz, respectively. The 3-dB fractional bandwidth of the second band is smaller compared to the first band. However, this is not our concern in this work. The very compact size is $7 \times 9 \times 0.787$ mm^3 and $8 \times 8 \times 0.787$ mm^3 for two versions. The use of only one OLR resonator in the circuit is considered a smart way to save space and reduce the overall size. The first band of D-BPF needs to have a very small size. Then, one OLR resonator bent around the first band area would be a good idea to achieve a compact size D-BPF. The proposed D-BPF is attractive for further development and study for applications in wireless communication systems.

Acknowledgments

This study was funded by project code MHN2022-01.23 from the Ha Noi Open University.

References

[1] MILLER, T., JERVIS, V., CHAN, Y. S., et al. GSMA. *Roadmaps for Awarding 5G Spectrum in the APAC Region*. 70 pages. [Online] Cited 2023-09-20. Available at: https://www.gsma.com/spectrum/wp-content/uploads/2022/04/Roadmaps-for-awarding-5G-spectrum-in-the-APAC-region.pdf

[2] ALNAHWI, F. M., AL-YASIR, Y. I. A., ABDULHAMEED, A. A., et al. A low-cost microwave filter with improved passband and stopband characteristics using stub loaded multiple mode resonator for 5G mid-band applications. *Electronics*, 2021, vol. 10, no. 4, p. 1–15. DOI: 10.3390/electronics10040450

[3] AL-YASIR, Y. I. A., OJAROUDI PARCHIN, N., ABDULKHALEQ, A., et al. Design, simulation and implementation of very compact dual-band microstrip bandpass filter for 4G and 5G applications. In *16th International Conference on Synthesis, Modeling, Analysis and Simulation Methods and Applications to Circuit Design (SMACD).* Lausanne (Switzerland), 2019, p. 41–44. DOI: 10.1109/SMACD.2019.8795226

[4] KHANI, H. I., EZZULDDIN, A. S. A survey on microstrip single/multiband bandpass filter for 5G applications. *Engineering and Technology Journal*, 2023, vol. 41, no. 2, p. 467–483. DOI: 10.30684/etj.2022.135858.1288

[5] YANG, R. Y., HON, K., HUNG, C. Y., et al. Design of dual-band bandpass filters using a dual feeding structure and embedded uniform impedance resonators. *Progress In Electromagnetics Research*, 2010, vol. 105, p. 93–102. DOI: 10.2528/PIER10042504

[6] ALKANHAL, M. A. S. Dual-band bandpass filters using inverted stepped-impedance resonators. *Journal of Electromagnetic Waves and Applications*, 2009, vol. 23, no. 8–9, p. 1211–1220. DOI: 10.1163/156939309789023411

[7] WANG, J. P., WANG, B. Z., WANG, Y. X., et al. Dual-band microstrip stepped-impedance bandpass filter with defected ground structure. *Journal of Electromagnetic Waves and Applications*, 2008, vol. 22, no. 4, p. 463–470. DOI: 10.1163/156939308784150335

[8] WENG, M. H., KAO, C. H., CHANG, Y. C. A compact dual-band bandpass filter using cross-coupled asymmetric SIRs for WLANs. *Journal of Electromagnetic Waves and Applications*, 2010, vol. 24, no. 2–3, p. 161–168. DOI: 10.1163/156939310790735679

[9] BOUFOUSS, R., NAJID, A. Design of microstrip dual-band bandpass filter for sub-6 GHz 5G mobile communications. *Jordanian Journal of Computers and Information Technology,* 2023, vol. 9, no. 4, p. 287–293. DOI: 10.5455/jjcit.71-1688749546

[10] ZHUANG, Z., HU, N., WU, Y., et al. Multi-transmission poles dual-band bandpass filter with extended bandwidth. In *IEEE MTT-S International Wireless Symposium (IWS).* Guangzhou (China), 2019, p. 1–3. DOI: 10.1109/IEEE-IWS.2019.8803942

[11] FU, S., WU, B., CHEN, J., et al. Novel second-order dual-mode dual-band filters using capacitance loaded square loop resonator. *IEEE Transactions on Microwave Theory and Techniques*, 2012, vol. 60, no. 3, p. 477–483. DOI: 10.1109/TMTT.2011.2181859

[12] ZHANG, Z., XIA, M., LI, G. Compact dual-band bandpass filter with high selectivity using stub-loaded stepped-impedance resonators. *Progress In Electromagnetics Research Letters*, 2022, vol. 102, p. 101–107. DOI: 10.2528/PIERL21112501

[13] SU, Y. K., CHEN, J. R., WENG, M. H., et al. A right slotted patch dual-mode dual band bandpass filter used for WLAN. *Microwave and Optical Technology Letters*, 2009, vol. 51, no. 2, p. 491–494. DOI: 10.1002/mop.24078

[14] XU, L. J., ZHANG, G., TANG, Y. M., et al. Compact dual-mode dual-band bandpass filter with wide stopband for WLAN applications. *Electronics Letters,* 2015, vol. 51, no. 17, p. 1372–1374. DOI: 10.1049/el.2015.1913

[15] IEU, W., ZHANG, D., ZHOU, D. High-selectivity dual-mode dual-band microstrip bandpass filter with multi-transmission zeros. *Electronics Letters*, 2017, vol. 53, no. 7, p. 482–484. DOI: 10.1049/el.2016.4103

[16] XU, J., XU, K. D., ZHANG, M., et al. Dual-band bandpass filter using two simple coupled microstrip rings. *Engineering Reports*, 2020, vol. 3, no. 2, p. 1–7. DOI: 10.1002/eng2.12288

[17] ZHANG, J., LIU, Q., ZHANG, D., et al. Design of compact high temperature superconducting dual-band filter using dual-composite right-/left-handed resonators. *Microwave and Optical Technology Letters*, 2021, vol. 63, no. 11, p. 2693–2698. DOI: 10.1002/mop.32936

[18] YUAN, W., REN, B., GUAN, X., et al. Compact dual-band balanced bandpass filter using CRLH resonator with intrinsic common-mode suppression and multiple transmission zeros. *AEU - International Journal of Electronics and Communications*, 2023, vol. 171, p. 1–6. DOI: 10.1016/j.aeue.2023.154881

[19] GARG, P., JAIN, P. Design and analysis of a bandpass filter using dual composite right/left handed (D-CRLH) transmission line showing bandwidth enhancement. *Wireless Personal Communications*, 2021, vol. 120, p. 1705–1720. DOI: 10.1007/s11277-021-08529-6

[20] SHEN, G., CHE, W., FENG, W., et al. Analytical design of compact dual-band filters using dual composite right-/left-handed resonators. *IEEE Transactions on Microwave Theory and Techniques*, 2017, vol. 65, no. 3, p. 804–814. DOI: 10.1109/TMTT.2016.2631168

[21] SHEN, G., WANG, X., CHE, W., et al. Miniaturized high-performance D-CRLH resonator and filter based on accurate equivalent circuit model. In *International Workshop on Electromagnetics: Applications and Student Innovation Competition (iWEM)*. Hsinchu (Taiwan), 2015, p. 1–3. DOI: 10.1109/iWEM.2015.7365026

[22] HSIEH, L. H., CHANG, K. Equivalent lumped elements G, L, C, and unloaded Q's of closed- and open-loop ring resonators. *IEEE Transactions on Microwave Theory and Techniques*, 2002, vol. 50, no. 2, p. 453–460. DOI: 10.1109/22.982223

[23] EVERYTHING RF. *TEM Wavelength Calculator*. 1 page. [Online] Cited 2023-09-20. Available at: https://www.everythingrf.com/rf-calculators/wavelength-calculator

[24] KIM, C., HYEON LEE, T., SHRESTHA, B., et al. Miniaturized dual-band bandpass filter based on stepped impedance resonators. *Microwave and Optical Technology Letters*, 2017, vol. 59, no. 5, p. 1116–1119. DOI: 10.1002/mop.30481

About the Authors …

Xuan Phuc DAO received the M.Sc. degree in Electronics and Telecommunications Engineering from Hanoi Open University, Hanoi, Vietnam. He is currently a Lecturer with the Faculty of Electrical and Electronic Engineering, Hanoi Open University. His research interests include signal processing in B5G/6G systems and ML/AI applications in big data processing.

Van Son NGUYEN (corresponding author) received the B.E. degree in Electrical Engineering and the M.S. degree in Electronics and Telecommunications Engineering from Hanoi Open University, Hanoi, Vietnam. He is currently a Lecturer with the Faculty of Electrical and Electronic Engineering, Hanoi Open University. His research interests include signal processing in 5G/6G systems and ML/AI applications in big data processing.

Van Dung TRAN received a Master of Electronic Engineering at Macquarie University in 2019. He is working as a team leader at the IMC institute in Vietnam. His expertise includes integrated circuit (IC) designs at the system level for satellite communications, high radio frequency integrated circuits designs (RFIC) and monolithic microwave integrated circuit (MMIC) designs in different processes.

The Hoang NGUYEN was born in 1993. He received his B.S. and M.S. degrees in Mechatronics and Robotics Engineering from Irkutsk National Research Technical University, Russia, in 2017 and 2019, respectively. He currently is a mechanical engineer at the Institute for Technology Development, Media and Community Assistance. His research interests include antenna and filter design modulation.

Xuan Loi DAI was born in 1991. He received his M.E in Electronic Engineering from Belarusian State University of Informatics and Radio Electronics in 2015. Currently he is a Ph.D. student at the Military Institute of Science and Technology in Vietnam. His research interests include RF design and signal processing.

Nghia Hoang TRONG was born in 1990. He graduated with a degree in Electronics and Telecommunication Engineering in 2013 and a master's degree in Electronic Engineering in 2018 at the Electric Power University. Currently, he is an expert at the Vietnam Research Institute of Electronics, Informatics and Automation. His research interests include internet, network protocol, network security, WSN, IoT.

Tran Tuan LINH is a student in the Faculty of Electrical and Electronic Engineering, Hanoi Open University. His research interests include telecommunication system, signal processing and modulation.